Force-detected electron-spin resonance:Adiabatic inversion, nutation, and spin echo

K. Wago,* D. Botkin, C. S. Yannoni, and D. Rugar
IBM Research Division, Almaden Research Center, 650 Harry Road, San Jose, California 95120
(Received 29 July 1997)

Electron-spin resonance of E' centers in vitreous silica was studied using force-detection techniques at temperatures down to 5 K. Cyclic adiabatic inversion of electron spins was performed by frequency modulation of the applied microwave magnetic field. This produced an oscillatory magnetic force between the electron spins and a nearby permanent magnet, resulting in the vibration of a cantilever on which the sample was mounted. By pulsing the microwave field prior to the force-detection sequence, nutation of the spins could be observed. Spin echoes were observed mechanically using a modified echo-pulse sequence. The decay of magnetization during cyclic adiabatic inversion was also studied and is discussed in terms of utility for future single-spin detection experiments. [S0163-1829(98)03702-3]

I. INTRODUCTION

Recent experimental work[1–10] has demonstrated sensitive detection of both electron-spin resonance (ESR) and nuclear magnetic resonance (NMR) using magnetic resonance force microscopy (MRFM).[11–14] In typical MRFM experiments, a kilohertz-frequency magnetic force is generated by using magnetic resonance to periodically modulate the sample magnetization in the presence of a strong magnetic-field gradient. The oscillatory force is then sensed via angstrom-scale vibration of a cantilever on which the sample is mounted.

In previous ESR-MRFM experiments, modulation of the sample magnetization has been accomplished by cyclic saturation using modulation of the microwave magnetic field B_1 and/or modulation of the polarizing field B_0.[1,15] Cyclic saturation implicitly depends on having an ensemble of spins whose relaxation time is much shorter than the modulation period, allowing the magnetization to saturate and recover nearly instantaneously as the sample is driven in and out of resonance. Since the concept of saturation relies on the behavior of an ensemble, cyclic saturation is not a suitable technique for future MRFM experiments directed towards the detection of individual electron spins.

An alternative modulation method that should be extendable to the single-spin level is cyclic adiabatic inversion, previously used for force-detected NMR in micron-size samples.[4] In cyclic adiabatic inversion, the spin magnetization is aligned either parallel or antiparallel to the effective field in the rotating frame, while the direction of the effective field is periodically inverted by modulating the frequency of the B_1 field. For cyclic adiabatic inversion to be effective, the rotating frame relaxation time[16] must be long enough for a large number of inversion cycles to be completed, allowing a measurable cantilever vibration to build up.

Achieving a sufficiently long relaxation time is problematic for electron spins at room temperature since relaxation times are commonly in the microsecond or nanosecond range. At low temperature, however, relaxation times are much longer and a number of electron spin systems exhibit sufficiently slow relaxation. We have chosen to investigate a particularly attractive system: E' centers in vitreous silica. E' centers are defect sites characterized by singly occupied silicon orbitals.[17] For spin densities on the order of 10^{17} cm^{-3}, E' centers are known to have T_1 relaxation times on the order of seconds at temperatures as high as 5–10 K.[18] Such long relaxation times are well suited for cyclic adiabatic inversion experiments.

The present work serves several purposes. First, we demonstrate that cyclic adiabatic inversion can indeed be used with an electron-spin system to generate a detectable oscillating force. After describing basic MRFM signals from E' centers, we show measurements of nonequilibrium magnetization states due to nutation and spin echoes. Finally, we study the relaxation behavior of E' centers during cyclic adiabatic inversion and measure the rate of magnetization decay as a function of the applied B_1 field. While the experiments presented here were performed using a micron-size sample containing millions of spins, we believe that the magnetization decay results, in particular, will be useful for planning future single-spin experiments. Related experiments on bulk samples have been carried out using a conventional ESR spectrometer modified to detect adiabatic rapid passage signals.[19]

II. FORCE DETECTED ESR

A. Experiment

The experiments were performed using a low-temperature magnetic resonance force detection apparatus[9,10] schematically shown in Fig. 1. The sample material was synthetic vitreous silica (Spectrosil) that was irradiated by ^{60}Co γ rays (4.4×10^8 rad) to produce E' centers.[20] The spin concentration was measured to be 3.5×10^{16}/cm^3 using a standard spin-counting technique.[19] The spin-lattice relaxation time T_1 was 1.5 s at 5 K. A sample piece with approximate dimensions 50 μm$\times$50 μm$\times$5 μm was glued onto a commercial single-crystal-silicon cantilever[21] with a spring constant $k\simeq0.07$ N/m and a mechanical-resonant frequency $f_c\simeq5.46$ kHz (with the sample loaded). Angstrom-scale motion of the cantilever was monitored by a fiber-optic interferometer[22] and synchronously detected with a lock-in amplifier. In order to speed up the cantilever response time, damping feedback was applied to the cantilever using a piezoelectric element.[4,23,24]

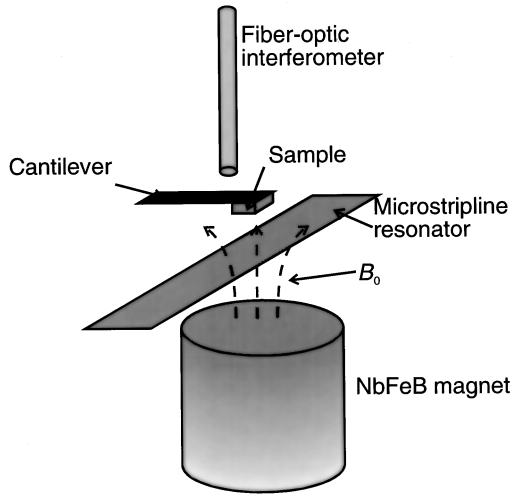

FIG. 1. Schematic setup of the experiment.

The sample was positioned 200 μm above the center of a microstripline resonator[10,25,26] that produced a microwave field B_1 at $\omega/2\pi=12.6$ GHz. The input power to the resonator ranged from 4 to 140 mW, corresponding to a B_1 strength of 0.23 to 1.35 G. The polarizing field B_0 was a combination of the homogeneous field from a superconducting magnet and the inhomogeneous field ($\sim$2300 G) produced by a permanent magnet located 800 μm away from the sample. The permanent magnet created a field gradient of 2 G/μm and served to generate a magnetic force on the sample. Due to the field gradient, only spins in a certain ''resonant slice'' satisfy the magnetic resonance condition, $\omega=\gamma B_0$, where γ is the electron gyromagnetic ratio. All experiments were performed at low temperature (5–10 K).

B. Cyclic adiabatic inversion

An oscillatory magnetic force from the resonant spins is generated by a ''probe sequence,'' which consists of frequency modulation of the microwave field such that $\omega(t)=\omega_0+\Delta\omega(t)$, where $\omega_0=\gamma B_0$. Starting with $\Delta\omega(0)=-2\pi\times 10$ MHz$\equiv-\Omega$, the microwave field is switched on and the frequency is modulated such that $\Delta\omega(t)=-\Omega\cos(2\pi f_c t)$. After several thousand cycles ($t=0.4$ s), the microwave field is switched off. Provided that the adiabatic condition[27] is satisfied during the probe sequence, this sequence induces cyclic inversion of the resonant magnetization **M**, which follows the direction of the rotating frame effective field[4]

$$\mathbf{B}_{\mathrm{eff}}(t)=B_1\hat{\mathbf{x}}-\frac{\Delta\omega(t)}{\gamma}\hat{\mathbf{z}}, \tag{1}$$

where $\hat{\mathbf{x}}$ and $\hat{\mathbf{z}}$ are the unit vectors in the rotating frame. Consequently, the longitudinal component of **M** oscillates at a frequency f_c, causing the cantilever to vibrate.

Figure 2(a) shows the cantilever-vibration amplitude during a typical probe sequence obtained at 5.2 K using a microwave input power of 4 mW ($B_1=0.23$ G). Damping feedback was set to give a cantilever response time of approximately 25 ms and a lock-in time constant of 3 ms was used. The signal was averaged over roughly 30 probe sequences, with 4 s between successive sequences to allow the spins to repolarize. As shown in Fig. 2(a), the cantilever vibrated in response to the probe sequence and a peak vibration amplitude of $\sim$1 Å-rms was achieved approximately 25 ms after the start of the sequence. After the initial peak, the amplitude decayed exponentially with a decay time constant of approximately 55 ms. This indicates that **M** decayed in magnitude while it was modulated by the probe sequence. Taking into account the cantilever response time and lock-in time constant, we estimate the decay time constant of the magnetization to be 25 ms. This magnetization decay will be discussed further in Sec. IV.

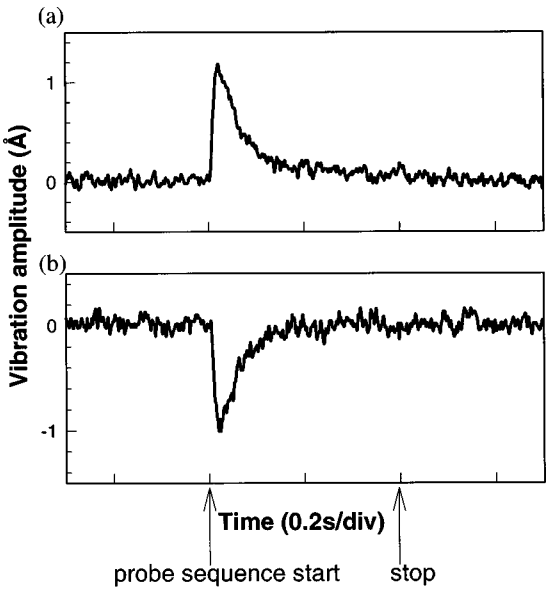

FIG. 2. (a) Time dependence of the cantilever-vibration amplitude. The start and stop of the probe sequence are indicated by arrows. The probe sequence consists of frequency modulation to the microwave field such that $\Delta\omega(t)=-\Omega\cos(2\pi f_c t)$, inducing cyclic adiabatic inversion of the electron-spin magnetization. The peak frequency deviation $\Omega/2\pi$ was 10 MHz. (b) Inverted cantilever response obtained when sample magnetization was adiabatically inverted by a frequency ramp before the probe sequence.

In order to verify that frequency modulation of B_1 indeed causes adiabatic inversion of **M**, we applied a single additional frequency ramp prior to the probe sequence. The microwave field was switched on with $\Delta\omega=\Omega$ and then ramped to $\Delta\omega=-\Omega$. This ramp should adiabatically invert **M**. The same probe sequence as before was then applied: $\Delta\omega(t)=-\Omega\cos(2\pi f_c t)$. As shown in Fig. 2(b), cantilever vibration was excited, but with opposite phase compared to the case in which only the probe sequence was applied. This indicates that the magnetization before the start of the probe sequence was indeed adiabatically inverted by the preparatory frequency ramp.

An ESR spectrum can be obtained by measuring the cantilever response to the probe sequence while sweeping the field from the superconducting magnet. Figure 3 shows the peak amplitude of the cantilever vibration as a function of B_0. The line shape is symmetric with a width of 12 G. This width, considerably broader than the intrinsic linewidth for E' centers,[28] results from the use of the large gradient with a sample of finite thickness and from the large FM deviation $\Omega/2\pi=20$ MHz ($\Omega/\gamma\simeq 7.1$ G).

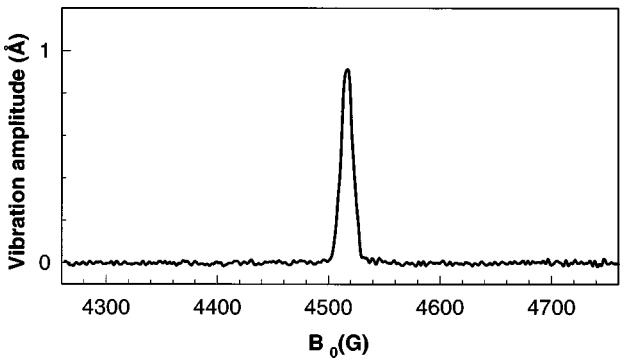

FIG. 3. Force-detected ESR spectrum. The peak amplitude of the cantilever vibration is plotted as a function of the polarizing field strength. The peak deviation $\Omega/2\pi$ was 20 MHz, the cantilever response time was $\sim$10 ms, and the signal was averaged over 50 scans. The peak appears when $B_0=\omega_0/\gamma$ at the sample position.

C. Steady-state magnetization during cyclic adiabatic inversion

While the peak amplitude of the cantilever vibration reflects the state of the magnetization just prior to the probe sequence, it is also interesting to investigate the steady-state cantilever vibration achieved at the end of the probe sequence. In Fig. 2, the cantilever-vibration amplitude decays almost to zero by the end of the probe sequence; however, we found that this is not always the case and that the steady-state amplitude depends on the strengths of both B_0 and B_1. Figure 4(a) shows the cantilever-vibration amplitude during the probe sequence with a microwave input power of 52 mW

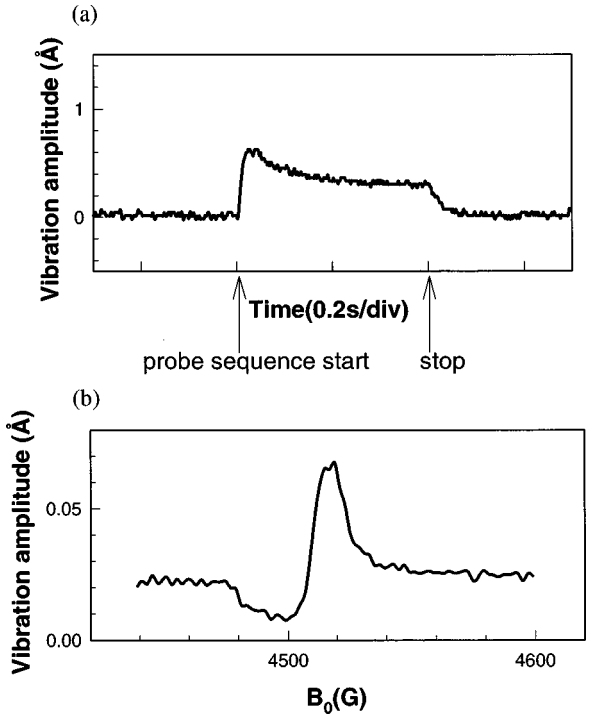

FIG. 4. (a) Time dependence of the cantilever-vibration amplitude with a microwave input power of 52 mW ($B_1=0.82$ G). The vibration amplitude reaches a steady-state value by the end of the probe sequence. (b) The steady-state cantilever-vibration amplitude as a function of the B_0 strength. Absolute vibration amplitude is smaller than in (a) because greater damping feedback was used.

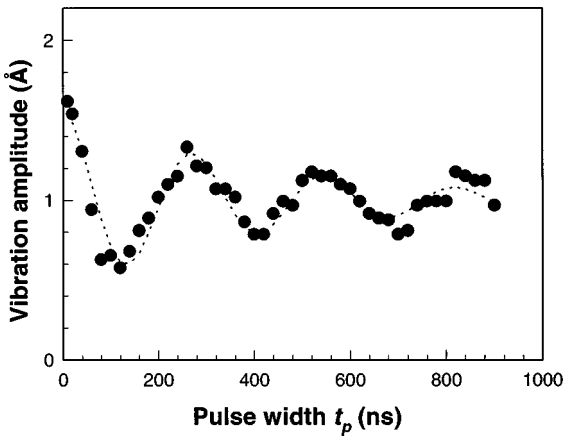

FIG. 5. Force-detected nutation signal. The peak amplitude of the cantilever vibration is plotted as a function of the width of a microwave pulse t_p applied prior to the probe sequence. A microwave power of 130 mW was used for the pulse, and 4 mW was used for the probe sequence. The dotted line is a fit to a damped cosinusoidal oscillation with an offset.

($B_1=0.82$ G). After the initial excitation, the vibration amplitude decays and reaches a steady-state value of approximately 0.3 Å rms.

The steady-state value of cantilever-vibration amplitude changes sign as the external field is swept, leading to the bipolar spectrum[29] shown in Fig. 4(b). The cantilever-vibration amplitude reaches a positive steady-state value when B_0 is slightly above resonance ($B_0-\omega/\gamma>0$), and a negative value when B_0 is below resonance ($B_0-\omega/\gamma<0$). These results can be understood in terms of spin dynamics in the rotating frame. In the steady state, **M** is locked parallel to $\mathbf{B}_{\rm eff}$ if $B_0-\omega/\gamma>0$ and antiparallel to $\mathbf{B}_{\rm eff}$ if $B_0-\omega/\gamma<0$.[16] When cyclically modulated by the FM sequence, the magnetization antiparallel to $\mathbf{B}_{\rm eff}$ generates an oscillatory force that is 180° out of phase with respect to that generated when **M** is parallel to $\mathbf{B}_{\rm eff}$.

III. NONEQUILIBRIUM MAGNETIZATION MEASUREMENTS

A. Nutation

The initial peak amplitude of the cantilever vibration reflects the state of longitudinal magnetization at the start of the probe sequence. This fact can be used to probe nonequilibrium states of magnetization.[8] To demonstrate this, we performed nutation and spin echo experiments.

Nutations can be measured by applying a microwave pulse of width t_p before the probe sequence. The pulse causes resonant spins to precess about $\mathbf{B}_{\rm eff}=B_1\hat{\mathbf{x}}$ in the rotating frame with an angular frequency γB_1. As a result, the longitudinal component of **M** is given by $M_z=M_0\cos(\gamma B_1 t_p)$, where M_0 is the thermal equilibrium magnetization. The probe sequence following the pulse generates an oscillatory force proportional to M_z that excites the cantilever vibration. Figure 5 shows the peak cantilever-vibration amplitude as a function of the microwave pulse width t_p. A microwave input power of 130 mW was used for the pulse and 4 mW was used for the probe sequence. The signals show an oscillation with a 270 ns period and

gradually decreasing amplitude. The oscillation is superimposed on a positive offset. Since the oscillation period corresponds to $2\pi/(\gamma B_1)$, the amplitude of B_1 for the 130 mW microwave pulse is determined to be 1.3 G. This result calibrates the B_1 field at the location of the sample generated by the microstripline resonator.

The positive offset is due to off-resonance spins in the sample (i.e., due to the field gradient and the finite sample thickness). With the frequency deviation $\Omega/2\pi = 10$ MHz used for the probe sequence, spins that are off-resonance by $|\Delta B| = \Omega/\gamma \simeq 3.6$ G still contribute to the force signal significantly.[5,8,9] Rather than precessing about $B_1\hat{\mathbf{x}}$, these off-resonance spins will precess in a cone about $\mathbf{B}_{\text{eff}} = B_1\hat{\mathbf{x}} + \Delta B\hat{\mathbf{z}}$, which is tilted 70° from the $\hat{\mathbf{x}}$ axis (for $B_1 = 1.3$ G). Spins precessing in this cone will always have a positive z component, leading to a positive offset in the nutation.

The decay of the nutation is also attributed to off-resonance spins. For the off-resonance case, the precession frequency $\gamma|\mathbf{B}_{\text{eff}}|$ differs from γB_1, causing spins in different regions of the sample to precess at different rates. The interference caused by a range of precession frequencies leads to a gradual decay of the oscillation amplitude in the total nutation signal. This effect dominates over the decay due to spin-spin relaxation processes (T_2 decay), which are related to the much smaller homogeneous broadening.

B. Spin echoes

Spin echoes play an important role in many magnetic resonance techniques. In conventional magnetic resonance, a $\pi/2$-τ-π pulse sequence is used to generate an echo. After the $\pi/2$ pulse, the spread in precession rates of the magnetization due to local fields and the inhomogeneity of B_0 causes a reversible decay of transverse magnetization. When a π pulse is applied after a time τ, spins are refocused at $t = 2\tau$, leading to an echo, the size of which is given by $M_0 \exp(-2\pi/T_2)$. Since the MRFM technique described here is sensitive to the longitudinal component of $\mathbf{M}$, the spin echo is detected by applying a $\pi/2$-τ-π-τ'-$\pi/2$ pulse sequence. The last $\pi/2$ pulse rotates the refocused magnetization to the longitudinal direction, which is mechanically detected by a subsequent probe sequence.

The experiment was carried out with the pulse sequence shown in Fig. 6(a). The peak amplitude of the cantilever vibration was measured while changing the time interval τ_A between the first $\pi/2$ pulse and the π pulse and keeping a fixed time interval τ_B between the two $\pi/2$ pulses. This has the effect of ''walking'' the echo through the last $\pi/2$ pulse. The widths of the $\pi/2$ and π pulses were 70 ns and 140 ns, respectively. Figure 6(b) shows the result for $\tau_B = 1$ μs. A peak is observed at $\tau_A \simeq 500$ ns $= \tau_B/2$, corresponding to the refocus condition for a spin echo.

The results for various τ_B are shown in Fig. 6(c). In each case, a peak appears when $\tau_A \simeq \tau_B/2$, representing spin echoes at various time intervals. With increasing τ_B, the peak height gradually decreases, presumably due to the T_2 decay as in conventional spin echo experiments.[30] The observed decay time indicates a T_2 on the order of 5 μs. For comparison, T_2 of 2.1 μs has been measured previously using conventional techniques on a silica sample containing a slightly higher concentration of spins.[31]

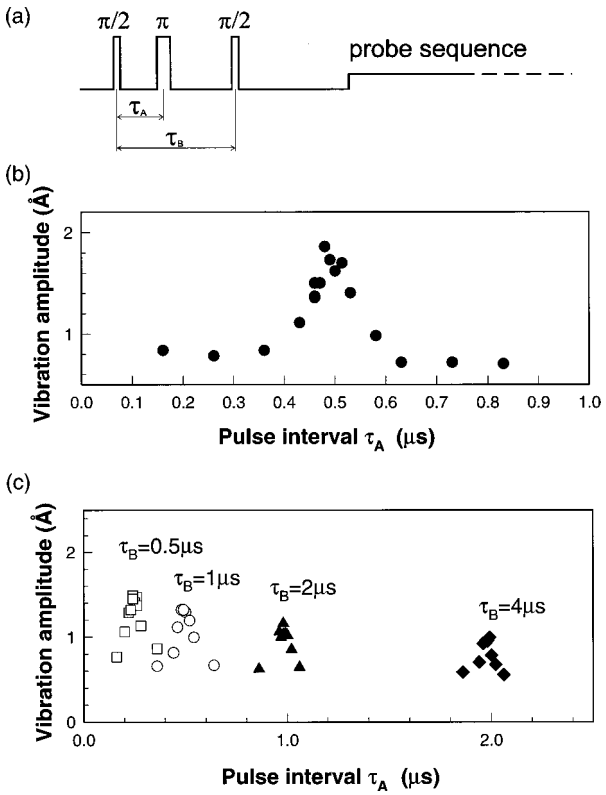

FIG. 6. (a) Pulse sequence used for the spin-echo experiment. A microwave power of 130 mW was used for the pulses, and 4 mW was used for the probe sequence. Widths of $\pi/2$ and π pulses were 70 ns and 140 ns, respectively. (b) The peak amplitude of the cantilever vibration as a function of τ_A, with a fixed $\tau_B = 1$ μs. A peak appears when $\tau_A \simeq \tau_B/2$, corresponding to a spin echo. (c) Spin echoes observed with various τ_B. The amplitude of the spin echoes gradually decreases as τ_B increases.

IV. MAGNETIZATION DECAY DURING ADIABATIC INVERSION CYCLES

One key issue for the force detection of electron spins is the relaxation rate of the spins while they are subjected to cyclic adiabatic inversion. As mentioned earlier, the magnetization decays during the force-detection sequence (Fig. 2). For a successful MRFM experiment, the spin magnetization must last long enough to excite the cantilever vibration to a detectable level. The decay of magnetization can be due to a variety of effects, including spin-lattice relaxation in the rotating frame, violation of the adiabatic condition, and spin-spin relaxation processes.

As shown in Fig. 7, the spin-lattice relaxation time in the rotating frame $T_{1\rho}$ can be measured by staying spin-locked on resonance for a variable time τ_{lock} before the probe sequence. The data in Fig. 7 shows the peak cantilever-vibration amplitude as a function of the spin-locking time for $B_1 = 0.23$ G. The signal decreases exponentially towards a steady-state value as τ_{lock} increases. The decay time constant was estimated to be $T_{1\rho} \simeq 190$ ms, in reasonable agreement with the value measured using conventional techniques.[19]

The observed magnetization decay time constant during repeated adiabatic reversals was found to be significantly shorter than $T_{1\rho}$. For example, the observed decay time constant in Fig. 2 was only 25 ms. To further investigate this effect, we used the trapezoidal FM wave form shown in Fig.

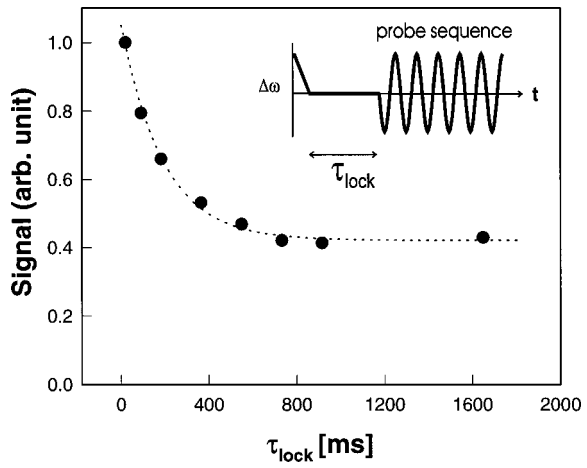

FIG. 7. The peak amplitude of the cantilever vibration as a function of the spin-lock time $\tau_{\rm lock}$ before the probe sequence. The dotted line is a fit to an exponential decay with an offset. The signal decays with a time constant $T_{1\rho}\simeq 190$ ms. The inset shows the FM wave form used for the measurement.

8, instead of the usual sinusoidal frequency modulation. The slope of the linear frequency ramp in the wave form was set such that $|\gamma^{-1}d\omega/dt|=|d\mathbf{B}_{\rm eff}/dt|=3.0\times 10^6$ G/s.

The frequency modulation of B_1 causes an oscillation of longitudinal magnetization such that

$$M_z(t)=\widetilde{M}(t)\,\frac{\Delta\omega(t)}{\sqrt{(\gamma B_1)^2+[\Delta\omega(t)]^2}}, \tag{2}$$

where $\widetilde{M}(t)$ is the magnitude of the magnetization, which varies slowly compared to the 5.5 kHz modulation frequency. The first harmonic Fourier component (in rms) of $M_z(t)$ is approximately given by $(2\sqrt{2}/\pi)\widetilde{M}(t)$ for a $\Delta\omega(t)$ with a trapezoidal wave form. If $\widetilde{M}(t)$ slowly decays such that $\widetilde{M}(t)=M_0\,\exp(-t/\tau_m)$, the rms amplitude of the resulting oscillatory force is given by

$$\widetilde{F}(t)=\frac{2\sqrt{2}}{\pi}M_0G\,\exp\left(-\frac{t}{\tau_m}\right)+\widetilde{F}_b, \tag{3}$$

where G is the field gradient and $\widetilde{F}_b$ is a small background oscillatory force that is included to account for spurious feedthrough of the microwave modulation.

The rms amplitude of the cantilever response $\widetilde{A}(t)$ is given by the convolution

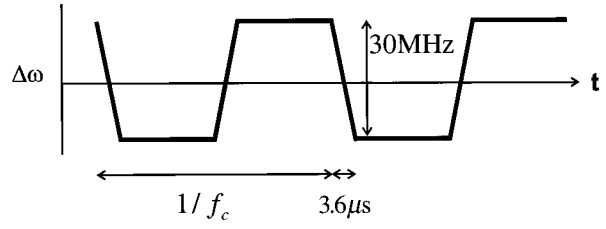

FIG. 8. Trapezoidal FM wave form used to study magnetization decay. The slope of the trapezoid is set such that $|\gamma^{-1}d\omega/dt|=|d\mathbf{B}_{\rm eff}/dt|=3.0\times 10^6$ G/s.

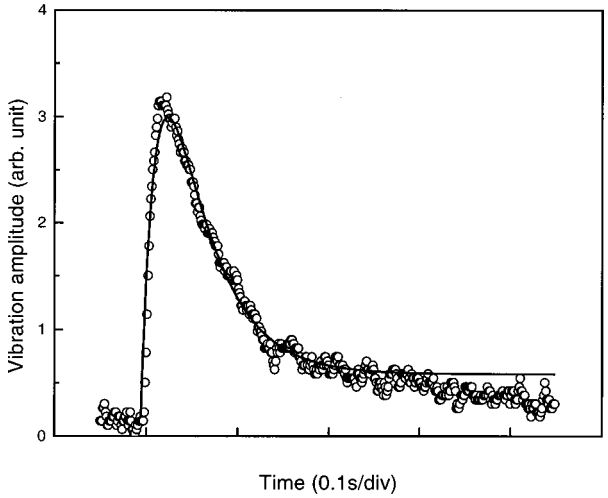

FIG. 9. A typical cantilever response for the trapezoidal modulation. The line is a fit using the function in Eq. (6). The magnetization decay time τ_m is found to be 46 ms in this case. $B_1=1.35$ G.

$$\widetilde{A}(t)=\int_0^t h(t')\widetilde{F}(t-t')dt', \tag{4}$$

where

$$h(t)=\frac{Q_{\rm eff}}{k\tau_c}\exp\left(-\frac{t}{\tau_c}\right) \tag{5}$$

is the impulse response function of the cantilever. Here, $Q_{\rm eff}$ and $\tau_c=Q_{\rm eff}/\pi f_c$ are the effective Q factor and $1/e$ response time of the cantilever, respectively, taking into account the damping feedback. Equations (3) and (4) lead to the cantilever response

$$\widetilde{A}(t)=\frac{Q_{\rm eff}}{k}\left\{\frac{2\sqrt{2}}{\pi}\,\frac{M_0G}{1-\tau_c/\tau_m}\left[\exp\left(-\frac{t}{\tau_m}\right)-\exp\left(-\frac{t}{\tau_c}\right)\right]+\widetilde{F}_b\left[1-\exp\left(-\frac{t}{\tau_c}\right)\right]\right\}. \tag{6}$$

A typical cantilever response for the trapezoidal modulation sequence is shown in Fig. 9. The observed cantilever response was fit to Eq. (6) using three adjustable parameters M_0, τ_m, and $\widetilde{F}_b$. The other parameters were determined independently. For Fig. 9, we found that $M_0=2.4\times 10^{-13}$ emu$=2.6\times 10^7\mu_B$, where μ_B is the Bohr magneton, and $\tau_m=46$ ms. The uncertainty in these results is estimated to be on the order of 10%.

Magnetization decay time constants τ_m obtained for various B_1 strengths are plotted in Fig. 10. Values of adiabaticity parameter[27] $\gamma B_1^2/|d\mathbf{B}_{\rm eff}/dt|$ are also indicated in the figure. It was found that τ_m increases as B_1 increases, suggesting that the magnetization decay is due to the violation of the adiabatic condition, $|d\mathbf{B}_{\rm eff}/dt|\ll\gamma B_1^2$. At the maximum B_1, where $\gamma B_1^2/|d\mathbf{B}_{\rm eff}/dt|\simeq 10$, $\tau_m=46$ ms and it appears to be reaching a plateau, indicating that loss due to nonadiabaticity is no longer dominant. Nevertheless, τ_m is still significantly shorter than $T_{1\rho}\simeq 190$ ms. An additional mechanism for magnetization decay, such as rotating frame cross-relaxation

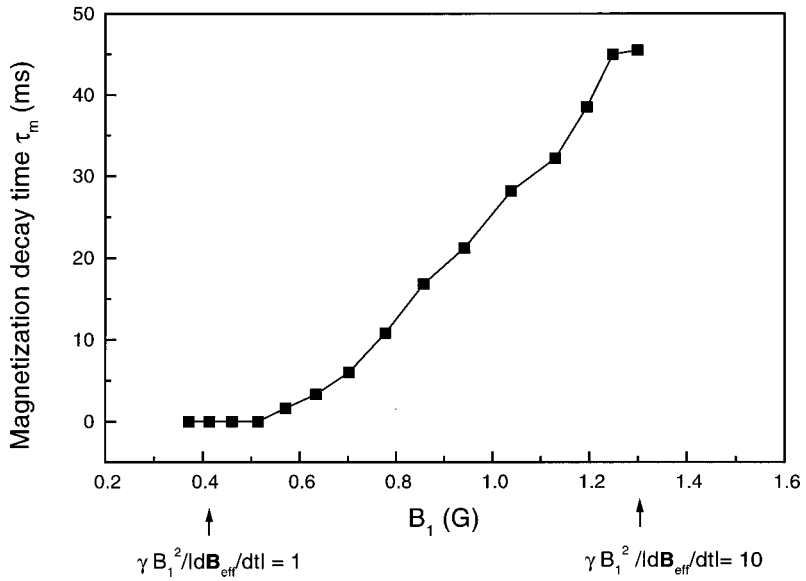

FIG. 10. Magnetization decay time τ_m as a function of B_1. Arrows indicate values of adiabaticity parameter $\gamma B_1^2/|d\mathbf{B}_{\rm eff}/dt|$.

processes among spins in inhomogeneously broadened lines, might be responsible for the relatively short τ_m.[19]

V. CONCLUSION

We have demonstrated force detection of ESR signals associated with the E' centers in γ-irradiated vitreous silica using cyclic adiabatic inversion. Frequency modulation of the microwave field cyclically inverted the electron-spin magnetization, resulting in angstrom-scale vibration of the cantilever. Using this technique, it was possible to measure nonequilibrium states of the magnetization, including electron spin nutations and spin echoes. The results presented here demonstrate that force detection is capable of a wide range of magnetic resonance experiments.

The decay during cyclic adiabatic inversion was also investigated and we found that, with sufficiently strong B_1, spin magnetization lasts on the order of 0.05 s, equivalent to approximately 250 adiabatic inversion cycles. This relatively long lifetime may have implications for future single-spin experiments since the spin lifetime determines the detection bandwidth that must be used. A sharp magnetic tip (50 nm radius) generates a field gradient on the order of 10 G/Å at a position $\sim$150 Å below the tip. For an electron spin located at this position and undergoing cyclic adiabatic inversion, the resulting interaction force is 7×10^{-17} N-rms. To detect such a small force in a detection bandwidth of 1/0.05 s$=$20 Hz, a force sensitivity of 2×10^{-17} N/$\sqrt{\rm Hz}$ or better is needed to achieve unity signal-to-noise ratio. Such force sensitivity was recently demonstrated using ultrathin single-crystal silicon cantilevers.[32] Assuming that the spin-relaxation time is not adversely affected by the close proximity of the magnetic tip, the long spin lifetime of E' centers make them a suitable candidate for future single-spin MRFM experiments.

ACKNOWLEDGMENTS

We thank D. L. Griscom for providing the Spectrosil sample material. We thank J. A. Sidles, H.-M. Vieth, and J. Wegener for helpful discussions and O. Züger for his many earlier contributions to this project. We also thank R. D. Kendrick for his technical help. This work was partially supported by the Office of Naval Research Contract No. N00014-95-C-0124.

*Also at Dept. of Applied Physics, Stanford University, Stanford, CA 94305. Electronic mail: wago@loki.stanford.edu

[1] D. Rugar, C. S. Yannoni, and J. A. Sidles, Nature (London) **360**, 563 (1992).
[2] O. Züger and D. Rugar, Appl. Phys. Lett. **63**, 2496 (1993).
[3] O. Züger and D. Rugar, J. Appl. Phys. **75**, 6211 (1994).
[4] D. Rugar, O. Züger, S. Hoen, C. S. Yannoni, H.-M. Vieth, and R. D. Kendrick, Science **264**, 1560 (1994).
[5] O. Züger, S. T. Hoen, C. S. Yannoni, and D. Rugar, J. Appl. Phys. **79**, 1881 (1996).
[6] K. J. Bruland, J. Kryzystek, J. L. Garbini, and J. A. Sidles, Rev. Sci. Instrum. **66**, 2853 (1995).
[7] P. C. Hammel, Z. Zhang, G. J. Moore, and M. L. Roukes, J. Low Temp. Phys. **101**, 59 (1995).
[8] O. Züger, S. T. Hoen, H.-M. Vieth, C. S. Yannoni, and D. Rugar (unpublished).
[9] K. Wago, O. Züger, R. Kendrick, C. S. Yannoni, and D. Rugar, J. Vac. Sci. Technol. B **14**, 1197 (1996).
[10] K. Wago, O. Züger, J. Wegener, R. Kendrick, C. S. Yannoni, and D. Rugar, Rev. Sci. Instrum. **68**, 1823 (1997).
[11] J. A. Sidles, Appl. Phys. Lett. **58**, 2854 (1991).
[12] J. A. Sidles, Phys. Rev. Lett. **68**, 1124 (1992).
[13] J. A. Sidles, J. L. Garbini, K. J. Bruland, D. Rugar, O. Züger, S. Hoen, and C. S. Yannoni, Rev. Mod. Phys. **67**, 249 (1995).
[14] C. S. Yannoni, O. Züger, D. Rugar, and J. S. Sidles, in *Encyclopedia of Nuclear Magnetic Resonance*, edited by D. M. Grant and R. K. Harris (Wiley, Chichester, 1996), pp. 2093–2100.
[15] In a related technique, torque-detected ESR, cyclic absorption of angular momentum from a microwave field was used. See, C. Ascoli, P. Baschieri, C. Frediani, L. Lenci, M. Martinelli, G. Alzetta, R. M. Celli, and L. Pardi, Appl. Phys. Lett. **69**, 3920 (1996).

[16] C. P. Slichter, *Principle of Magnetic Resonance*, 3rd ed. (Springer-Verlag, Berlin, 1990), pp. 242–244.
[17] D. L. Griscom, Nucl. Instrum. Methods Phys. Res. B **1**, 481 (1984).
[18] J. G. Castle, Jr. and D. W. Feldman, J. Appl. Phys. **36**, 124 (1963).
[19] C. S. Yannoni, R. D. Kendrick, H.-M. Vieth, J. Wegener, and D. Rugar (unpublished).
[20] The authors thank D. L. Griscom for generously providing this material.
[21] Model ESP(W), Digital Instruments Inc., Santa Barbara, CA 93117.
[22] D. Rugar, H. J. Mamin, and P. Guethner, Appl. Phys. Lett. **55**(25), 2588 (1989).
[23] J. Merts, O. Marti, and J. Mlynek, Appl. Phys. Lett. **62**, 2344 (1993).
[24] K. J. Bruland, J. L. Garbini, W. M. Dougherty, and J. A. Sidles, J. Appl. Phys. **80**, 1959 (1996).
[25] W. J. Wallace and R. H. Silsbee, Rev. Sci. Instrum. **62**, 1754 (1991).
[26] H. How, A. Widom, and C. Vittoria, IEEE Trans. Microwave Theory Tech. **39**, 660 (1991).
[27] A. Abragam, *The Principles of Nuclear Magnetism* (Oxford University Press, London, 1961), p. 66.
[28] R. A. Weeks and C. M. Nelson, J. Appl. Phys. **31**, 1555 (1960).
[29] The small background signal of ~ 0.02 Å observed for field values far from resonance is due to spurious microwave-feedthrough effects.
[30] E. L. Hahn, Phys. Rev. **80**, 580 (1950).
[31] S. S. Eaton and G. R. Eaton, J. Magn. Reson., Ser. A **102**, 354 (1993).
[32] T. D. Stowe, K. Yasumura, T. Kenny, T. Botkin, K. Wago, and D. Rugar, Appl. Phys. Lett. **71**, 288 (1997).